Melting Kinetics of Polymer Crystals with an Entropic Barrier

Akihiko Toda,*,† Isao Kojima,‡ and Masamichi Hikosaka†

Graduate School of Integrated Arts and Sciences and Graduate School of Biosphere Science, Hiroshima University, 1-7-1 Kagamiyama, Higashi-Hiroshima 739-8521, Japan

Received September 27, 2007; Revised Manuscript Received October 22, 2007

ABSTRACT: The melting behaviors of polyethylene and poly(vinylidene fluoride) have been experimentally examined by thermal analysis, optical microscopy, and atomic force microscopy. The melting velocity is found to show a nonlinear dependence on the degree of effective superheating. The dependence clearly suggests the existence of an activation barrier, though crystal melting is generally supposed to proceed without any barriers. The behavior has been reproduced by a Monte Carlo simulation of the entropic barrier of pinning proposed by Sadler and Gilmer for chain-folded crystallization of polymers.

Introduction

On the basis of general understanding, the melting of crystals will not be limited by any activation barriers, since the crystal−melt interface of the majority of materials is supposed to be thermally rough. Even for flat interface of the rest including polymer crystals, the crystal corners are liable to melt without the cost of new extra surfaces, namely, without the activation barrier of nucleation. The kinetics is therefore believed to be only limited by thermal diffusion and has been regarded as a trivial example of transport phenomena. The purpose of the present report is to suggest a counterexample of this biased view with the melting of polymer crystals and to indicate that the basic understanding is quite primitive.

As a typical example of complex soft-matter, crystalline polymers exhibit various complex behaviors in the so-called melting region, such as intrinsically broad temperature region of melting of chain-folded crystals and the parallel occurrence of melting, recrystallization, and reorganization.[1] The melting condition also influences the relaxation of chains in the molten state, i.e., the degree of entanglement in the molten state, which has significant influence on the subsequent crystallization and the properties of the final structures.[2,3] Those behaviors basically originate in the metastability of chain-folded crystals, which will also influence the melting kinetics.

Measurement of melting rate of polymer crystals is not an easy task because of the following characteristics. First, polymer crystallization from the melt evolves as an aggregate, e.g., spherulite, of tiny lamellar crystallites in the micron scale. The melting of these crystallites takes place simultaneously everywhere in the aggregate, and hence the melting rate cannot be determined as the shrinkage velocity of the aggregate (Figure 1). On the other hand, in terms of isolated crystals in the bulk, it is difficult to prepare them and the melting has been believed to be too fast for the direct observation by microscopy.

Due to these difficulties, melting of polymer crystals has been examined by indirect methods, such as thermal analysis. Actually, there is a long history of the study of melting by thermal analysis with the pioneering work of Wunderlich's group,[1] whose results suggested an unusual behavior of melting kinetics indicating a nonlinear dependence of the melting rate on superheating.[4] In our recent examinations of the melting kinetics in response to a periodic modulation in temperature[5−8] and to linear heating,[7,8] we have concluded that the "total" rate of melting, R, nonlinearly depends on the effective superheating, $\Delta T = T_s - T_M$, where T_s and T_M represent the sample temperature and the melting point of the examined crystals with chain folding, respectively; $R(\Delta T) \propto \Delta T^y$ with $1 < y$. With ultrafast heating (ca. $>10^2$ °C/s), similar results have also been reported in a recent work by Minakov et al.[9] The nonlinear dependence indirectly suggested an activation barrier in the melting kinetics. For the confirmation of the results, we need direct measurement of the propagation velocity of melting interface in a single crystal, which is the main subject of the present paper. In order to circumvent the difficulties and to ensure the detailed microscopic observation of single crystals, we prepared single crystals in a relatively thin melt film (several micron thick) and applied almost instantaneous temperature jump for melting.

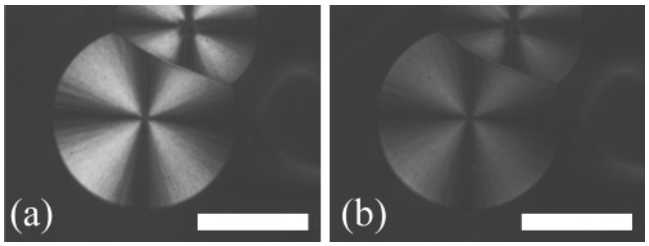

Figure 1. Evolution of the melting of PVDF spherulites with gradual decrease in the contrast from (a) to (b) on heating at 10 °C/min taken by POM. The temperature difference is 2 °C between (a) and (b). Bar represents 100 μm.

In the following, we first examine the experimental results on melting by thermal analysis and by direct measurements of single crystals in a thin melt film to confirm the nonlinear dependence of the melting rate of polymer crystals on the degree of effective superheating. Then, we discuss possible activation processes and propose that an entropic barrier of melting will be the only possible mechanism of the activation barrier for melting. As one of possible entropic barriers, we examine the effect of pinning barrier on the melting kinetics by Monte Carlo simulation.

Experimental Section

Polymers examined are polyethylene, PE (NIST SRM1483, $M_w = 32\,100$ and $M_w/M_n = 1.11$), and poly(vinylidene fluoride),

* To whom correspondence should be addressed. Email: atoda@hiroshima-u.ac.jp. Phone: +81-82-424-6558. Fax: +81-82-424-0757.
† Graduate School of Integrated Arts and Sciences.
‡ Graduate School of Biosphere Science.

10.1021/ma702162m CCC: $40.75
Published on Web 12/08/2007

PVDF (KF1000, $M_w = 2.5 \times 10^5$ and $M_w/M_n = 2.1$, Kureha Chemical Industries).

First, for the thermal analysis by differential scanning calorimetry (DSC), a Q100 (TA Instruments) was used for all measurements. Nitrogen gas with a flow rate of 20 mL min^{-1} was purged through the cell. The reference pan was removed in all experiments to reduce the number of uncontrollable parameters.[10]

In order to see the superheating effect in the melting of polymer crystals by constant heating rate (conventional DSC, CDSC), it is necessary to avoid recrystallization and reorganization. For this purpose, samples were annealed near the melting temperature to increase the perfection (and thickness) of crystals and minimize the change in melting point on subsequent heating runs. PE was crystallized by cooling at 10 °C/min from 150 to 100 °C and then annealed at 130 °C for 3 h. Similarly, PVDF was initially crystallized by cooling at 10 °C/min from 210 to 120 °C to grow crystals of the α form.[11] Then, the α-form crystals were partially melted at 176 °C, crystallized at 170 °C for 90 min, and annealed at 176 °C for 24 h. It is known that the high temperature annealing of PVDF for longer time interval causes solid−solid conversion of α to γ form starting mainly from existing γ-form crystals.[12] Because of the self-seeding of the α-form crystals, we did not see the higher melting peak of the γ form, while the annealing was necessary to minimize the reorganization at slow heating rates. It is also to be noted that for the measurements of PVDF with periodic modulation in temperature (temperature-modulated DSC, TMDSC) we did not apply the high temperature annealing, as mentioned below, because we can differentiate the melting from recrystallization and reorganization with the TMDSC due to the difference in their responses to the periodic modulation in temperature.[5] The results of CDSC and TMDSC agree well with each other as shown in the Results and Discussion section, and hence the influence of the conversion will be quite small even if it exists.

After the thermal treatments, samples were heated at 0.2, 0.8, 2, 4, 7, 11, 17, and 26 °C/min to see the shift in the endothermic peaks. In general, the shift in the melting peaks is attributable to the effects of superheating, thermal contact resistance between the bottom of the sample pan and its stage, and the temperature gradient in the sample. In order to minimize the thermal contact resistance, we applied silicone grease (Archer, 276-1372) between the surfaces. By doing this, we have confirmed that the thermal contact resistance became less than 10^{-3} KW^{-1}.[8] In comparison with the resistance of about 10 KW^{-1} with nitrogen purge gas,[8] the value could be practically negligible. Then, in order to examine the effect of the temperature gradient, we have examined PE samples with thicknesses of 20−100 μm and evaluated the degree of true superheating.

Second, for the TMDSC measurements, we have crystallized PE and PVDF with the same conditions as those for CDSC. For PVDF, we did not apply the high temperature annealing for the reason mentioned above. In TMDSC, we apply periodic temperature modulation to the constant underlying heating to examine the response appearing in the modulated heat flow. Basically, the response is expressed as a heat capacity of the complex quantity, $\tilde{C}e^{-i\alpha}$, determined by the ratio of the amplitudes of modulations in temperature, $\tilde{T}_s$, and heat flow, $\tilde{Q}$, and by the shift in phase angle between the modulations, ϵ and δ, as follows:

$$\tilde{C}e^{-i\alpha} \equiv \tilde{C}' - i\tilde{C}'' = \frac{\tilde{Q}}{\omega \tilde{T}_s} e^{-i(\epsilon - \delta)} \quad (1)$$

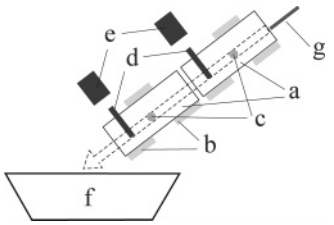

Figure 2. Schematic illustration of the sliding hot cells: (a) hot cell, (b) heater, (c) thermocouple, (d) stopper, (e) electromagnet, (f) coolant, and (g) sample.

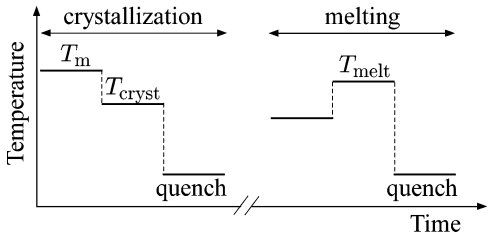

Figure 3. Temperature protocol in the plot against time. The temperature jumps were performed by the sliding hot cells shown in Figure 2.

where ω represents the angular frequency of the periodic modulation, i.e., $\omega = 2\pi/(\text{period})$. For a relaxation process such as glass transition and for first-order phase transitions, the response of the processes appears as the effective heat capacity having nonzero imaginary part. The present analysis utilizes the response of the melting transition. We have examined a modulation period of 13−100 s with the modulation amplitude adjusted for the condition of heating only, $dT_s/dt > 0$ ($\tilde{T}_s < \beta/\omega$), where the underlying heating rate, β, was 0.2, 0.4, 0.8, 1.6, and 3.2 °C/min. It is known that the magnitude and phase angle of the effective heat capacity are influenced by the modulation period in a systematic way with a larger deviation for a shorter period. Because of the negligible thermal contact resistance between the bottom of sample pan and its stage with the application of silicone grease, the calibration of the magnitude and phase angle can be simplified.[8] The magnitude is adjusted outside the transition region by multiplying a constant ratio to match the value at the longest period of 100 s, and for the phase angle, we subtract the value outside the transition region as the baseline. By doing this, the deviation from the more detailed calibration is 5−15% for the periods of 100−13 s.[8] The precision is good enough to examine the melting kinetics in a logarithmic scale as is done in the Results and Discussion section.

For the direct examination of the melting of PE single crystals, we prepared the single crystals embedded in a thin film (5−10 μm) on a cover glass by melting at 139 °C for 1 min and subsequent isothermal crystallization at 128.5 °C for 30 min. The samples were then quenched to a coolant of freezing isopentane kept at around −160 °C (Figure 3). By this procedure, single crystals of 30 μm long on average are embedded in the surrounding thinner crystallites and amorphous portions formed on quenching. The quenched amorphous portions were transparent so that the length and width of single crystals in the film could be measured by phase-contrast optical microscopy (OM, BX51, Olympus Corp.).

In order to apply temperature jumps in a shorter time interval for the crystallization and melting experiments, we applied the following two methods. In the first method, we set up a pair of hot cells made of brass connected to each other with a small gap (2 mm), as shown in Figure 2. The thin film sample on a cover glass slid down the cells set at different temperatures and

finally jumped into the coolant. By this method, the samples reached isothermal condition within a second, as shown in Figure 12. We applied this method for both of crystallization and melting.

In the first method, after the preparation and measurement of single crystals, the film was again dropped into the hot cell set at the melting temperatures of 132−137 °C, kept for a certain time interval for isothermal melting, and then quenched in the coolant to stop melting. The length and width of the same single crystals were measured again to examine the change in size on melting.

In the second method, the samples with single crystals prepared by the first method were slid into a hot stage (Mettler FP82) on a glass slide for the in situ measurement of the melting process by OM. With this method, due to low thermal conductivity of the glass slide, it took about 10 seconds to reach the isothermal condition, as typically shown in Figure 13.

After these procedures, in order to examine the fine details after melting, we applied chemical etching for PE[13] to reveal the single crystals by the selective removal of the portions formed on quenching. The single crystals were then examined by atomic force microscopy (AFM, SPI3800N, Seiko Instruments Inc.) in the dynamic mode.

For α-form PVDF crystals, we first prepared the α-form crystals by melting at 210 °C for 1 min and crystallization at 130 °C for 3 min. Then, the samples were again melted at 173.5 °C for 1 min, isothermally crystallized at 169 °C for 90 min, and finally quenched with the coolant kept at around −160 °C. For PVDF, we applied only the first method described above because of the weaker contrast of PVDF single crystals by OM. For examination by AFM, samples were then immersed in dimethylacetamide for 2 h at room temperature to remove the quenched portions.

Results and Discussion

By thermal analysis using DSC, we can evaluate the total rate of melting of the polymer crystallites, R. The rate of first-order phase transition, in general, is a function of the distance from the transition temperature ΔT, namely, the degree of superheating in the case of melting. With faster heating rate β, ΔT of each crystallite becomes larger in a shorter time interval, and hence the time interval of melting of each crystallite, τ_c, becomes shorter. The dependence of τ_c on the underlying heating rate, β, is therefore determined by the ΔT dependence of the melting rate, R, and hence the dependence of $R(\Delta T)$ can be evaluated from the dependence of $\tau_c(\beta)$.

The characteristic time, τ_c, is related to the shift in the peak temperature, ΔT_{shift}, of the superheating effect. The following relationship has been confirmed theoretically and experimentally:[7,8,14]

$$R(\Delta T) \propto \Delta T^{y} \tag{2}$$

$$\Delta T_{shift}(\beta) = T_s^{peak}(\beta) - T_s^{peak}(0) \cong \beta\tau_c(\beta) \propto \beta^{z} \tag{3}$$

$$z = \frac{1}{y+1} \tag{4}$$

where y is a constant, characterizing the melting kinetics.

Figure 4 shows the experimental results of the heating rate dependence of the endothermic peak on melting of the PE crystals, and Figure 5 shows the heating rate dependence of the melting peak temperature of PE and PVDF crystals. In the present experiments, by applying silicone grease between the bottom surface of the sample pan and its stage, the thermal contact resistance between them can be reduced to be negligibly small.[8] Therefore, the shift shown in Figure 5 is mostly due to the effects of superheating and the temperature gradient in the sample. As seen in Figure 5, thicker samples actually have larger apparent shift due to larger thermal lag in the sample. Present results confirm that a thickness of less than 45 μm will be thin enough for the evaluation of the true peak shift due to superheating for the examined range of heating rate (≤26 °C/min).

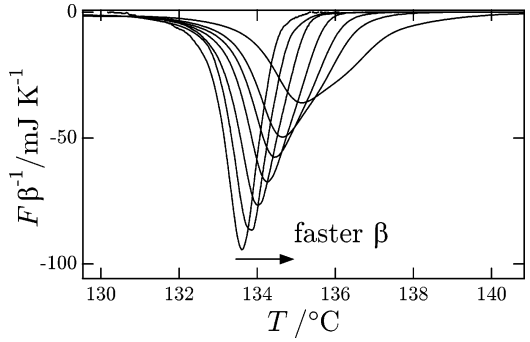

Figure 4. Heating rate dependence of the endothermic heat flow on melting of PE crystals obtained by DSC by heating at constant rates of β =0.2, 0.8, 2, 4, 7, 11, 17, and 26 °C/min. The endothermic peak shifts to higher temperature for faster heating. The heat flow has been normalized for heating rate. Sample thickness was 20 μm.

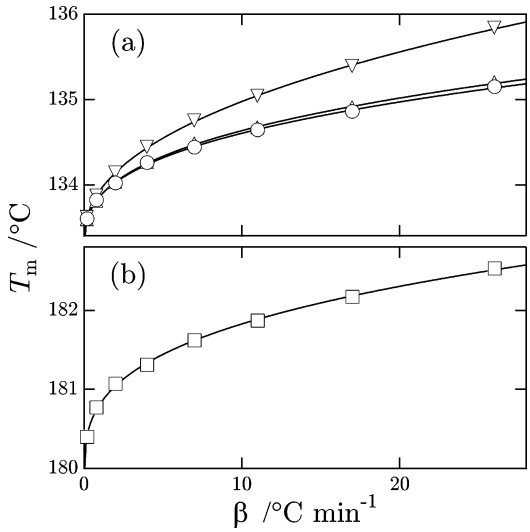

Figure 5. Heating rate dependence of the melting peak temperatures of (a) PE and (b) PVDF crystals. Sample thicknesses of PE in (a) were 20 (○), 45 (△), and 89 μm (▽), and sample thickness of PVDF in (b) was 31 μm. The power, z, values of the fitting lines are 0.35, 0.35, and 0.43 for 20, 45, and 89 μm thick samples of PE in (a), respectively, and 0.31 for PVDF in (b).

From the dependence of the melting peak on the heating rate shown in Figure 5, the fitting to the expression of eq 3 gives $T_s^{peak}(0)$ and z as the fitting parameters. From the power, z, the superheating dependence of the total rate of melting of each crystallite is evaluated as follows on the basis of eqs 2 and 4:

$$\Delta T_{shift} \propto \beta^{0.35} \rightarrow R \propto \Delta T^{1.9} \text{ for PE} \tag{5}$$

$$\Delta T_{shift} \propto \beta^{0.31} \rightarrow R \propto \Delta T^{2.3} \text{ for PVDF} \tag{6}$$

The ΔT dependence of the melting rate, $R(\Delta T)$, can also be evaluated from the frequency dependence of the effective heat capacity obtained from the heat flow in response to a periodic temperature modulation added to the constant heating rate, i.e.,

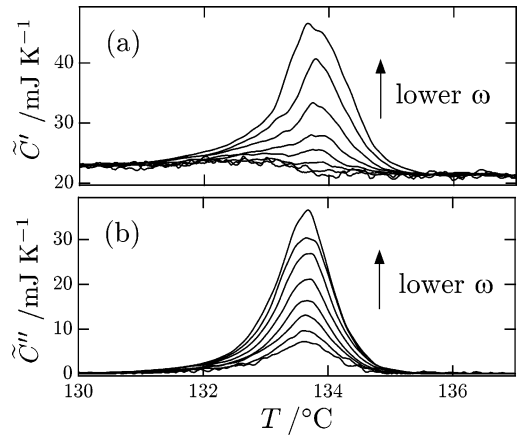

Figure 6. Typical frequency dependence of the effective heat capacity of complex quantity in the melting region of PE. The modulation periods are 13, 17, 22, 28, 36, 47, 60, and 78 s. The underlying heating rate was 0.4 °C/min.

a method of TMDSC. For the kinetics of first-order phase transition of a system composed of small domains (crystallites) having broad distribution of transition points, such as the case of polymer melting, the response of the kinetics to the periodic modulation in temperature, i.e., in ΔT, appears in the effective heat capacity, $\tilde{C}e^{-i\alpha}$, obtained by TMDSC in the following manner:

$$\tilde{C}e^{-i\alpha} \cong C_p + \frac{-\bar{F}/\beta}{1 + i\omega\tau_m(\beta)} \tag{7}$$

$$\tau_m(\beta) \propto |\beta|^{-x} (\propto \tau_c(\beta)) \tag{8}$$

$$x = \frac{y}{y+1} \tag{9}$$

where C_p represents the true heat capacity under constant pressure representing the heat capacity of the sample, $\bar{F}$ the underlying heat flow of transition kinetics, and τ_m the characteristic time corresponding to the mean time required for the completion of transition of each domain (crystallite). Due to the same reason as the shift of superheating for faster heating rate with conventional DSC, the characteristic time depends on the underlying heating rate, β. Therefore, by examining the β dependence of the characteristic time τ_m, the ΔT dependence of transition rate can be evaluated from the power x on the basis of eqs 2 and 9.

Figure 6 shows the typical experimental results of the frequency dependence of the effective heat capacity. Figure 7 shows the frequency dependence of the effective heat capacity at the melting peaks overlapped by the shift factor τ_m depending on the underlying heating rate, β; the shift factor is shown in the double logarithmic plots of Figure 8. From the slopes of the straight lines in Figure 8, the superheating dependence of the total rate of melting of each crystallite is evaluated as follows:

$$\tau_m \propto \beta^{-0.60} \rightarrow R \propto \Delta T^{1.5} \text{ for PE} \tag{10}$$

$$\tau_m \propto \beta^{-0.72} \rightarrow R \propto \Delta T^{2.6} \text{ for PVDF} \tag{11}$$

The results of CDSC and TMDSC on the power, y, of the ΔT dependence of R agree well with each other, and the value is lower for PE than for PVDF with both the methods. It is also to be noted that the present result with fractionated PE

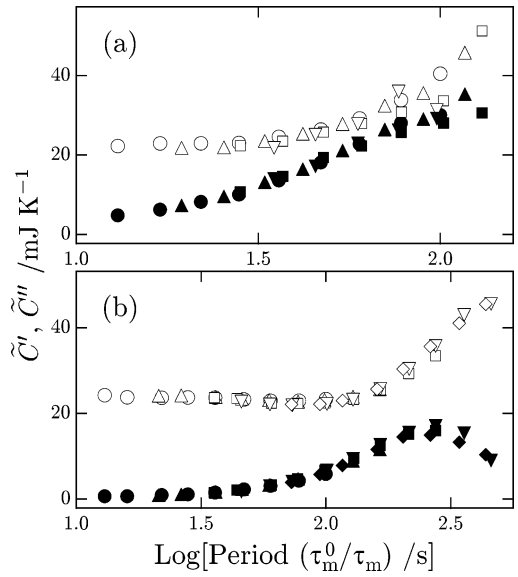

Figure 7. Frequency dependence of the effective heat capacity at the melting peaks of (a) PE and (b) PVDF: real part (open symbols) and imaginary part (filled symbols). The modulation periods are 13−100 s. β = 0.2 (○, ●), 0.4 (△ ▲), 08. (□, ■), 1.6 (▽, ▼), and 3.2 °C/min (◇, ♦). The data points are overlapped with the shift factor τ shown in Figure 8, τ_m^0 for 0.2 °C/min.

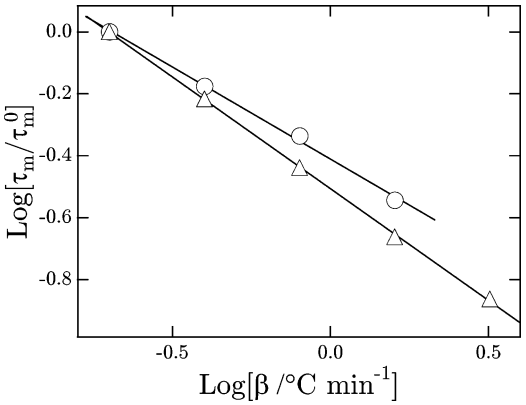

Figure 8. Double logarithmic plots of the characteristic time, τ_m, for PE (○) and PVDF (△) against β. τ_m is determined as the shift factor to overlap the data points in Figure 7, τ_m^0 for 0.2 °C/min. The slopes of the straight lines are −0.60 for PE and −0.72 for PVDF.

agrees well with our previous results using PE having broad molecular weight distribution, which have been concluded both from CDSC and from TMDSC after the deconvolution of the thermal contact resistance (without the application of silicone grease).[7] The power, y, of the ΔT dependence of the melting rate, R, has been supposed to be influenced by the chain mobility in the crystals, and hence the smaller value applies to PE, in which chains are expected to be mobile.[7] In order to confirm the conclusion obtained by the indirect methods of CDSC and TMDSC, we directly examine the melting of polymer single crystals grown from the melt in the following.

Figures 9 and 10 show the AFM images of crystals of PE and PVDF, respectively, kept at the melting temperature for the respective time intervals. It is to be noted that these are different crystals because we had to apply the etching technique (for PE) or the solvation technique (for PVDF) to remove the quenched portions for each sample to be examined by AFM. These crystals represent the typical size and shape of the crystals undergoing the melting. As is clearly seen in these images, the melting of crystals embedded in the bulk proceeds from the outer edge by shrinking in size. This observation for the crystals

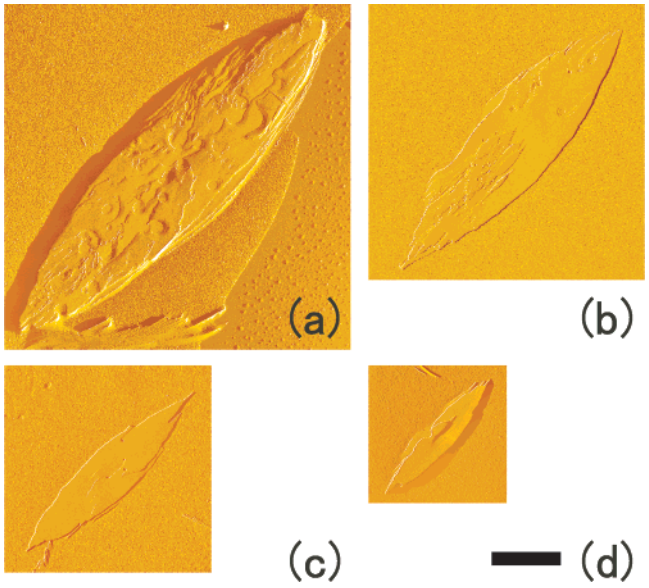

Figure 9. AFM amplitude images of PE crystals: (a) grown from the melt at 128.5 °C and melted at 134.5 °C for (b) 5 s, (c) 10 s, and (d) 15 s. The images are on the same scale and the bar represents 5 μm. Samples were chemically etched to reveal the crystals.[13]

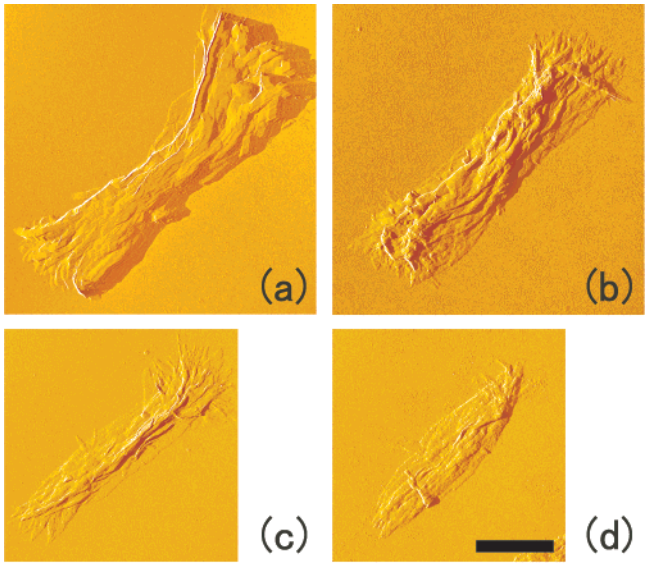

Figure 10. AFM amplitude images of PVDF crystals: (a) grown from the melt at 169.0 °C and melted at 180.0 °C for (b) 3 s, (c) 7 s, and (d) 10 s. The images are on the same scale and the bar represents 5 μm. Samples were immersed in dimethylacetamide to remove quenched portions.

in the bulk is in great contrast to a number of reports on single crystals placed on a substrate; for the crystals on the substrate, annealing and melting usually result in the creation of holes with thickened peripheries.[15] It is most probable that the surrounding melt prevents the formation of holes for the crystals in the film. For this reason, it is essential to examine the melting in the bulk and not on a substrate or the surface of the melt.

By AFM, we have also measured the thickness of these crystals at the edge from the height difference at the terraces of lamellae. As shown in Figure 11, the thickness at the crystal edge was almost constant for the melting time, $t > 0$. It means that we can neglect the thickening of crystals during the melting. Actually, we have chosen the crystallization temperature to be high enough to have the thick lamellae suppressing further thickening. In Figure 11, it is also seen that the edge of PE crystals is thinner before melting ($t = 0$) than during the course

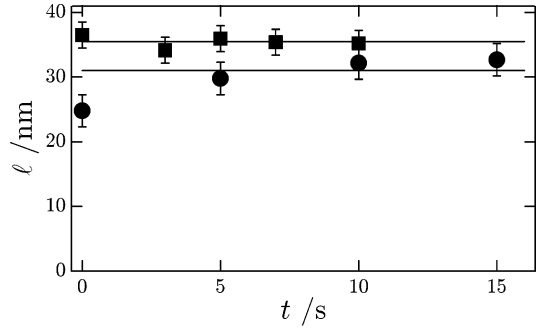

Figure 11. Lamellar thickness, *l*, at the edge of the crystals of PE (●) and PVDF (■) plotted against melting time. The set temperatures were 134.5 °C for PE and 180.0 °C for PVDF. The horizontal lines are the guides to the eye.

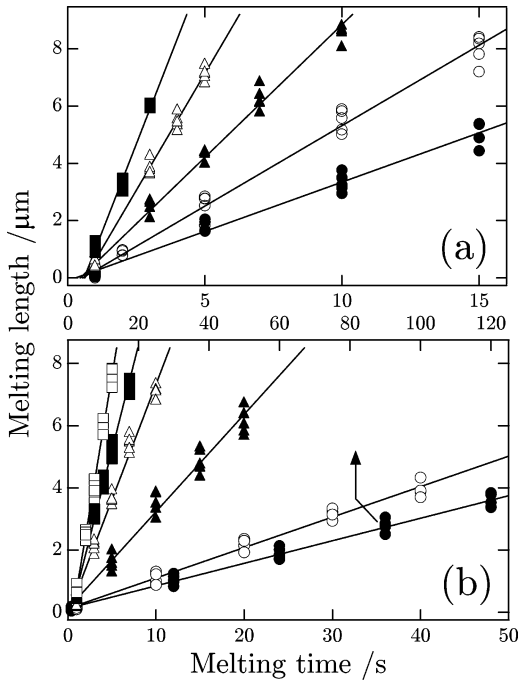

Figure 12. The changes in the length of the long axis of (a) PE and (b) PVDF crystals on melting in the sliding hot cell. The setting temperatures were 134.0 (●), 134.5 (○), 135.0 (▲), 135.5 (△), and 136.0 °C (■) in (a) and 177.5 (●), 178.0 (○), 179.0(▲), 180.0 (Δ), 180.5 (■), and 181.0 °C (□) in (b).

of melting ($t > 0$). It means that the PE crystals had a tapered shape near the edge ($\lesssim 1\mu$m) of the original crystals. In order to avoid the influence of this thickness change, we determined the melting velocity from the crystals which have already melted to a depth longer than 1 μm.

Figures 12 and 13 show the changes in length of single crystals with the melting time at the respective temperatures, measured by optical microscopy before and after the melting. The size change is proportional to the melting time from the time interval of 1 s with the sliding hot cell in Figure 12 and from the interval of 10 s for the Mettler hot stage in Figure 13, and the change in the width showed similar behavior. It means that the quench was successful and the isothermal melting rate is constant for the examined time intervals and temperatures. Below the temperatures shown in Figures 12 and 13, e.g., at 133.5 °C for PE and at 177.0 °C for PVDF, the melting of crystals proceeded to a certain depth and gradually ceased, as shown in Figure 14. We did not include the melting velocity in these temperature ranges, <133.5 °C for PE and <177.0 °C for PVDF. In the temperature ranges shown in Figures 12 and

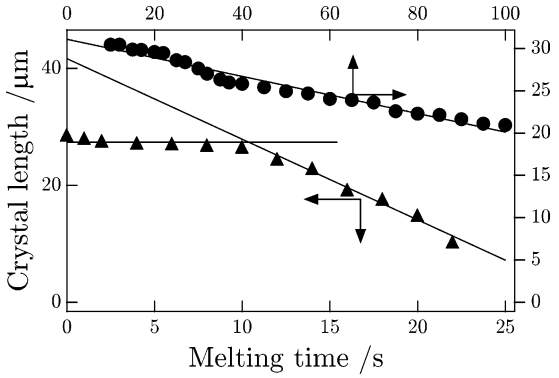

Figure 13. The changes in the length of the long axis of PE crystals on melting in the Mettler hot stage set at 134.0 (●) and 135.0 °C (▲).

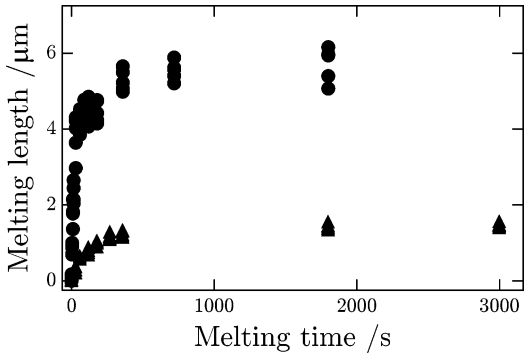

Figure 14. The changes in the length of the long axis of PE (●) and PVDF (▲) crystals on melting in the sliding hot cell set at 133.5 and 177.0 °C, respectively.

13, the crystals continued melting up to at least 1/3 of their original sizes.

Figure 15 shows the plots against temperature of the melting velocity in the directions of long and short axes. Nonlinear dependence of the velocity on temperature is clearly seen in Figure 15. The dependence on the set temperature, T_s, is translated to the dependence on the effective superheating, $\Delta T = T_s - T_M$. Therefore, the results confirm the nonlinear dependence on superheating of the melting velocity, V. The fitting of the curves gives the following expressions:

$$V \propto \Delta T^{2.1} \text{ for PE} \tag{12}$$

$$V \propto \Delta T^{3.3} \text{ for PVDF} \tag{13}$$

The power of nonlinearity, y, is larger for PVDF than for PE in agreement with the results of thermal analysis, indicating stronger nonlinearity for less mobile polymer chains in the crystalline state. The difference in the absolute values of y obtained by the thermal analysis and by the direct observation is partly due to the difference in the definition of the power in these methods; the power is for the total rate of melting in the thermal analysis and for the melting velocity in the direct observation.

The nonlinear dependence definitely suggests the existence of an activation barrier for melting. As mentioned in the Introduction section, we can rule out the possibility of surface nucleation for the melting from the outer edge. This also applies to the molecular nucleation,[16] which is also supposed to proceed on the lateral crystal surfaces. We have also confirmed that the melting does not proceed with the nucleation of holes in the crystals. It is to be further noted that the melting velocity shows strong anisotropy in the directions of long and short axes for both PE and PVDF crystals, as shown in Figure 15. The

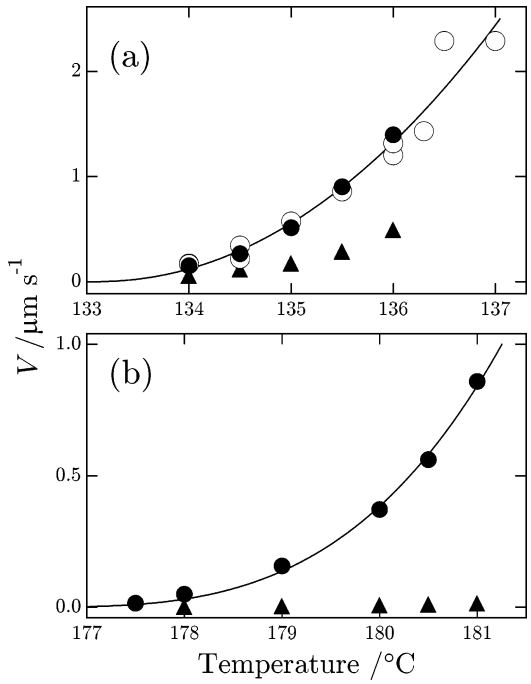

Figure 15. Plots of melting velocity, V, against setting temperature of (a) PE and (b) PVDF in the directions of long (●, ○) and short (▲) axes. The open symbols in (a) represent the rates obtained by the Mettler hot stage, and the closed ones represent the rates obtained by the sliding hot cell. The fitting curves in (a) and (b) are $V \propto (T - 133.0)^{2.1}$ and $V \propto (T - 176.3)^{3.3}$, respectively.

anisotropy suggests that the rate determining process differentiates the lateral surfaces of different crystal indexes. Therefore, there must be an unknown activation process at the "crystal−melt" interface. As a possible candidate, we can think of an entropic barrier[17−21] associated with the internal degree of freedom of flexible polymer chains at the melting front. There will be various possible routes of crystal melting with entropic barriers owing to a vast amount of conformational freedom of polymers. In the present report, we suggest one of the possibilities based on the entropic barrier of pinning,[18−21] which has been proposed as a possible activation barrier of polymer crystallization with chain folding.

Monte Carlo Simulation

The entropic barrier of pinning was originally proposed by Sadler and Gilmer[18−21] as an alternative model of chain-folded crystallization to the standard model based on surface nucleation process. The pinning represents a trap formed by an array of crystalline stems shorter than the critical thickness, l^*, below which crystallization does not proceed due to the excess free energy of chain folding. At the growth front, these stems form the pinning region, which becomes quasi-stable because of the entropic gain by varying the stem length without the creation of extra side surfaces (the shaded regions of Figure 16a). A similar situation is realized in the one-dimensional step on the growth face of small molecules (Figure 16b). The one-dimensional step is thermally rough at finite temperatures, and the rough growth front of the step corresponds to the pinning region. The one-dimensional step of small molecules can be propagated in the forward and backward directions without restriction. Concerned with the pinning region of polymers, however, due to the connectivity of these stems by the folded chains, the pinning region must be taken off for the propagation of the growth front, and this process limits the rate of propagation. It has been suggested by Monte Carlo simulations[18,20] and a rate equation approach[19,21] that the pinning model

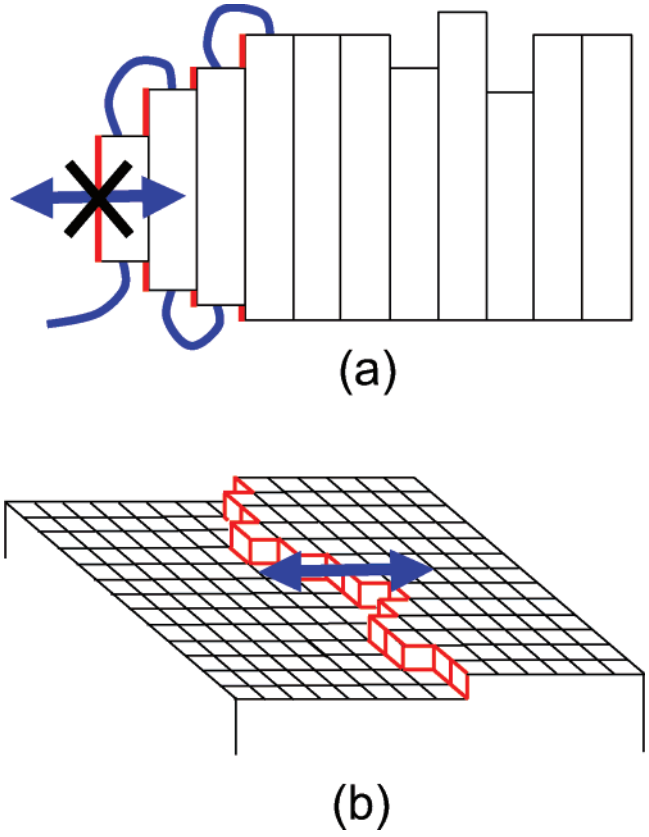

Figure 16. Schematic illustrations of (a) pinning region at the edge of one layer of the chain-folded crystal and (b) one-dimensional step on the crystal surface of small molecules.

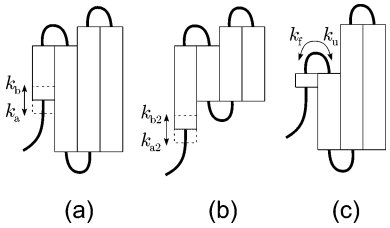

Figure 17. Processes at the melting/crystallization tip of a stem: advance and reverse processes for the stem shorter (a) and longer (b) than the preceding stem, and the processes of folding and unfolding in (c).

can reproduce the supercooling dependence of lamellar thickness, i.e., period of chain folding, and the crystal growth rate similar to those predicted by the standard model of Lauritzen and Hoffman.[22] However, despite the potential possibility of the pinning model, the similarity in the predictions of both the pinning and standard models prevented the judgment of the applicability, and the pinning model has not been seriously considered by others.

Concerned with melting, namely, the backward propagation of the edge, we expect that the entropic barrier of pinning will also be activated for a certain range above the crystallization temperature of the chain-folded crystals. Then, the nonlinear dependence of the melting velocity on the effective superheating, ΔT, may be explained by the pinning barrier. With this expectation, we have examined the behavior by a Monte Carlo simulation as follows.

We prepared a crystalline layer of stem length, l, and examined the backward propagation of the edge. We have assumed that the elementary processes occur only at the tip of the stem located at the edge, namely, we prohibited the

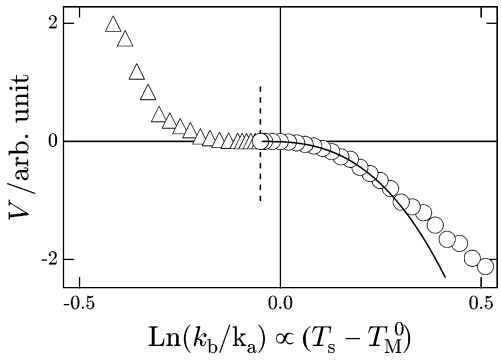

Figure 18. Plots of backward (melting, ○) and forward (crystallization, △) propagation velocities, V, obtained from the Monte Carlo simulation for $\exp[-\sigma/kT] = 0.01$ and $\exp[-q/kT] = 0.5$. The melting velocity is for $l = 10$ units, which melt at k_b/k_a larger than the broken line corresponding to T_M. The fitting line is $V \propto (T_s - T_M)^{2.7}$.

reorganization process within the crystalline layer. The elementary processes occur at the rates k_x (Figure 17); (a) k_a and k_b, addition and removal of a growth unit, (c) k_f and k_u, folding and unfolding of a chain, and (b) k_{a2} and k_{b2}, addition and removal of a growth unit at the edge with the penalty of creating new side surfaces. The probabilities of events and the corresponding time increments in the simulation were calculated from the rates, k_x, by the algorithm simulating stochastic events described by a Poisson distribution.[23]

Then, we assume that the rates satisfy the detailed balance, as follows:

$$\frac{k_b}{k_a} = \exp\left[-\frac{\Delta g}{kT}\right] \tag{14}$$

$$\frac{k_f}{k_u} = \frac{k_a}{k_b}\exp\left[-\frac{q}{kT}\right] \tag{15}$$

$$\frac{k_{a2}}{k_{b2}} = \frac{k_a}{k_b}\exp\left[-\frac{\sigma}{kT}\right] \tag{16}$$

where Δg represents the decrease in Gibbs free energy by the crystallization of a growth unit, q the free energy increase by chain folding, and σ the free energy increase by the addition of a growth unit at the edge with new side surfaces. For melting, the examined temperature, T_s, is above the melting temperature of the folded-chain crystals, T_M, but can be below the equilibrium melting point of an ideal crystal with fully extended chains, T_M^0; i.e., $T_M < T_s < T_M^0$. Then, at the set temperature, the crystalline layer with thickness, l, begins to melt when $l < l^* \equiv q/\Delta g$; here, l^* represents the critical stem length compensating for the free energy increase by chain folding, q, and Δg is defined as $\Delta g = \Delta h_f(T_M^0 - T_s)/T_M^0$, with Δh_f being the heat of fusion per unit volume of crystal.

Figure 18 shows the results of the Monte Carlo simulation for the backward propagation (melting) and forward propagation (crystallization) velocities of the edge, V. The curves in Figure 18 clearly indicate the nonlinear dependencies of the melting velocity and the crystallization velocity expected for the entropic barrier of pinning. The specific value of the power of the fitting line, e.g., 2.7 in Figure 18, is dependent on the choice of the parameters and the range of the fitting data, and hence we will not discuss the quantitative examination of the value in comparison with our experimental results for PE and PVDF. Actually, as seen in Figure 18, the dependence gradually shifts to linear dependence with vanishing effect of the pinning barrier at higher temperatures above T_M^0.

In the Monte Carlo simulation, we have allowed the addition and removal of a growth unit only at the tip of the stem located at the edge of the crystalline layer; this means that the reorganization in the crystalline stems was prohibited in the simulation. In reality, polymer crystals can undergo reorganization in the temperature range of melting, depending on the mobility of polymer chains in the crystalline state. For example, PE chains are supposed to be mobile in the crystalline state above the temperature of crystal dispersion at around 100 °C and can undergo thickening in the melting region.[15] The rate shows an exponential dependence on the lamellar thickness, i.e., slower thickening for thicker lamellae, and the thickness changes in proportion to the logarithm of annealing time under the isothermal condition. For the mobile chains in the crystalline state, the pinning region at the edge of crystalline layer does not have to be removed for the propagation of the edge. Instead of removal, the pinning region can be propagated in the forward and backward directions by chain sliding in the pinning region. If the chain sliding can occur without any barrier, the pinning mode mentioned in the above cannot be the rate determining process of melting or crystallization. We think that the easiness of chain sliding in the crystalline state actually influences the power of ΔT dependence on V, which was smaller for PE than that for PVDF. In order to consider the effects, the present modeling is too primitive because the purpose of the simulation is only to show the possibility of the nonlinear dependence on the effective superheating of the melting velocity with the entropic barrier. We need more realistic modeling for the quantitative examination of the results.

In the final part of the discussion, we need to mention a recent suggestion by Minakov et al.[9] on the nonlinear dependence of melting rate by a mechanical acceleration due to the difference in the thermal expansion between the crystal and the melt. We think, at ultrafast heating rates (ca. $>10^2$ °C/s) examined by the authors, the elastic strain may have a considerable influence on the kinetics for the melting completed in a very short time interval, and the effect may be the reason for the constant power of $z \simeq 0.2$ for all polymers examined. We suppose that the strain can be relaxed with relatively slow melting at a low degree of superheating, as applied in the present experiments, so we think that the entropic barrier will be the only influential factor for melting, depending on the dynamic nature of polymers in the crystalline state.

Conclusion

We have examined the melting behaviors of PE and PVDF crystals by thermal analysis and by direct observation with OM and AFM. By thermal analysis of the heating rate dependence of the melting peaks of CDSC and the characteristic time of TMDSC, we have reconfirmed that the total rate of melting shows a nonlinear dependence on superheating; $R \propto \Delta T^{1.9}$ (CDSC) and $\Delta T^{1.5}$ (TMDSC) for PE, and $R \propto \Delta T^{2.3}$ (CDSC) and $\Delta T^{2.6}$ (TMDSC) for PVDF. On the other hand, by examining the isothermal melting of crystals in the bulk with OM and with AFM after chemical etching or dissolving quenched portions, we have experimentally confirmed that the melting proceeds by the shrinkage of crystals from outside with constant melting velocity, which is in accordance with the results of in situ observation of melting of edge-on lamellae on a melt surface by AFM.[24,25] The melting velocity depends on the degree of superheating with the power of $V \propto \Delta T^{2.1}$ for PE and $V \propto \Delta T^{3.3}$ for PVDF.

These experimental results strongly suggest an activation process for melting. The possibility of a nucleation barrier can be excluded basically for the melting from outside and for the creation of holes experimentally. We suppose that an entropic barrier will be the most probable candidate for the activation process. On the basis of the entropic barrier of pinning suggested for the chain-folded crystallization by Sadler and Gilmer, we have examined the Monte Carlo simulation of melting and confirmed that the nonlinear dependence can be reproduced by this model. We think that the pinning model will be one of the possible mechanisms of entropic barrier, and hence further experimental and theoretical examination will be required for the quantitative analysis of the melting kinetics.

Note Added in Proof. It has come to the authors' notice that, for low molecular weight poly(ethylene oxide), the melting velocity of once-folded and extended chain crystals shows an exponential dependence on the gree of superheating. The behavior is in accordance with the present results for higher molecular weight polymer crystals of polyethylene and PVDF with multiple chain folding and thus suggests unique feature of melting of long chain molecules, in general.[26]

Acknowledgment. This work was partially supported by MEXT Japan, Grant-in-Aid for Scientific Research on Priority Areas, "Creation of Nonequilibrium Soft Matter Physics".

References and Notes

(1) Wunderlich, B. *Macromolecular Physics*; Academic Press: New York, 1976; Vol. 3.
(2) Rastogi, S.; Lippits, D. R.; Peters, G. M.; Graf, R.; Yao, Y.; Spiess, H. *Nat. Mater.* **2005**, *4*, 635
(3) Lippits, D. R.; Rastogi, S.; Höhne, G. W. H. *Phys. Rev. Lett.* **2006**, *96*, 218303
(4) Hellmuth, E.; Wunderlich, B. *J. Appl. Phys.* **1965**, *36*, 3039.
(5) Toda, A.; Tomita, C.; Hikosaka, M.; Saruyama, Y. *Thermochim. Acta* **1998**, *324*, 95.
(6) Toda, A.; Arita, T.; Tomita, C.; Hikosaka, M. *Polymer* **2000**, *41*, 8941.
(7) Toda, A.; Yamada, K.; Hikosaka, M. *Polymer* **2002**, *43*, 1667.
(8) Toda, A.; Hikosaka, M. *Thermochim. Acta* **2005**, *436*, 15.
(9) Minakov, A. A.; Wurm, A.; Schick, C. *Eur. Phys. J.* **2007**, *E23*, 43.
(10) Hatta, I.; Muramatsu, S. *Jpn. J. Appl. Phys.* **1996**, *35*, L858.
(11) Lovinger, A. J. In *Developments in Crystalline Polymers*; Bassett, D. C., Ed.; Applied Science Publishers: London, 1982; Vol. 1, Chapter 5.
(12) Lovinger, A. J. *Polymer* **1980**, *21*, 1317.
(13) Olley, R. H.; Hodge, A. M.; Bassett, D. C. *J. Polym. Sci., Polym. Phys. Ed.* **1979**, *17*, 627.
(14) Schawe, J. E. K.; Strobl, G. R.; *Polymer* **1998**, *39*, 3745.
(15) Geil, P. H. *Polymer Single Crystals*; John Wiley: New York, 1963.
(16) Wunderlich, B.; Mehta, A. *J. Polym. Sci., Part B: Polym. Phys.* **1974**, *12*, 255.
(17) Kundagrami, A.; Muthukumar, M. *J. Chem. Phys.* **2007**, *126*, 144901.
(18) Sadler, D. M.; Gilmer, G. H. *Polymer* **1984**, **25**, 1446.
(19) Sadler, D. M.; Gilmer, G. H. *Phys. Rev. Lett.* **1986**, *56*, 2708.
(20) Sadler, D. M. *Nature* **1987**, **326**, 174.
(21) Sadler, D. M.; Gilmer, G. H. *Phys. Rev.* **1988**, *B38*, 5684.
(22) Hoffman, J. D.; Davis, G. T.; Lauritzen, J. I., Jr. In *Treatise on Solid State Chemistry*; Hannay, N. B., Ed.; Plenum Press: New York, 1976; Vol. 3, Chapter 7.
(23) Voter, A. F. *Phys. Rev.* **1986**, *B34*, 6819.
(24) Beekmans, L. G. M.; van der Meer, D. W.; Vansco, G. J. *Polymer* **2002**, *43*, 1887.
(25) Hobbs, J. K. *Polymer* **2006**, 5566.
(26) Kovacs, A. J.; Gonthier, A.; Straupe, C. *J. Polym. Sci., Part C* **1975**, *50*, 283.

MA702162M